designs

MDPI

Article

Technical and 2E Analysis of Hybrid Energy Generating System with Hydrogen Production for SRM IST Delhi-NCR Campus

Shilpa Sambhi [1], Himanshu Sharma [1,*], Vikas Bhadoria [2], Pankaj Kumar [1], Georgios Fotis [3] and Lambros Ekonomou [4,*]

[1] Department of Electrical and Electronics Engineering, SRM Institute of Science and Technology, Delhi-NCR Campus, Ghaziabad 201204, Uttar Pradesh, India; shilpasambhi@gmail.com (S.S.); pankajkumar903106@gmail.com (P.K.)
[2] Industry Integration Cell, Shri Vishwakarma Skill University, Palwal 121102, Haryana, India; vikasbhadoria@gmail.com
[3] Department of Electrical and Electronics Engineering Educators, ASPETE—School of Pedagogical and Technological Education, 141 21 N. Heraklion, Greece; gfotis@gmail.com
[4] UBITECH Energy Sprl, 367 Avenue Louise, B-1050 Brussels, Belgium
* Correspondence: himanshuresearch58@gmail.com (H.S.); lekonomou@ubitech.eu (L.E.)

Abstract: This work intends to perform technical and 2E (economic & environmental) analysis for the proposed hybrid energy generating system for a part load at SRM IST at the Delhi-NCR campus, India. The investigation has been done for electricity generation and hydrogen production through renewable energy sources, mainly solar energy. It is in line with the Indian Government's initiatives. The proposed hybrid system has to meet the electric load demand of 400 kWh/day with a peak load of 74.27 kW and hydrogen load demand of 10 kg/day with a peak demand of 1.86 kg/h. The analysis has been performed for both on-grid and off-grid conditions. As a result, optimum results have been obtained off-grid condition, with \$0.408 per kWh cost of energy, \$16.6 per kg cost of hydrogen, low O&M cost (\$21,955 per year), a high renewable fraction (99.8%), and low greenhouse emissions (247 kg/year). In addition, sensitivity analysis has been performed between—(1) the solar PV array size & the number of battery strings, with NPC, renewable fraction & CO_2 emissions as sensitivity variables, and (2) reformer capacity & hydrogen tank capacity, with NPC as sensitivity variable.

Keywords: hybrid power plant; cost of energy; net present cost; green hydrogen; reformer; electrolyser

Citation: Sambhi, S.; Sharma, H.; Bhadoria, V.; Kumar, P.; Fotis, G.; Ekonomou, L. Technical and 2E Analysis of Hybrid Energy Generating System with Hydrogen Production for SRM IST Delhi-NCR Campus. *Designs* **2023**, *7*, 55. https://doi.org/10.3390/designs7020055

Academic Editors: Surender Reddy Salkuti and Dibin Zhu

Received: 18 March 2023
Revised: 6 April 2023
Accepted: 7 April 2023
Published: 9 April 2023

1. Introduction

Most economists and international organizations have realized the importance of sustainable energy in people's lives. It may ensure a better quality of life regarding health and economic independence in various countries. The world's electricity consumption is estimated to grow by 2.3% per year from 2015 to 2040 [1]. Worldwide power plants still use fossil fuels to fulfil about 80% of the electricity demand, threatening the rising levels of greenhouse gas, carbon dioxide (CO_2), levels [2]. The rise in CO_2 levels increases the average temperature globally, adversely affecting the global climate. In December 2015, world leaders decided to put a limit on the increase in global level to 2 °C at the Conference of the Parties, in short, called COP21 [3]. The burning of fossil fuels not only produces CO_2 but also other harmful gases like sulphur dioxide (SO_2), nitrogen oxides (NOx), and particulate matter. To accelerate the shift towards renewable energy sources (RES) for electricity generation, many countries like Denmark, Sweden, Norway, Italy, New Zealand, Canada, and Great Britain have started imposing carbon tax [4]. Due to recent technological advancements and high availability, solar energy is the most promising means to produce electricity [5]. The countries experiencing high wind speeds also use wind energy to produce electricity [6]. Another RES is hydro-kinetic energy, which uses speed of naturally flowing in river streams or man-made waterways to produce electricity [7].

Different strategies, like using locally available renewable sources for electricity generation, combined heat & power installations, and designing buildings with energy efficiency, have been adopted by European Union to reduce greenhouse gas [8]. European Union has set targets for national emissions in a year, electricity generation using RES and carbon capture & storage [9]. A Canadian company, Carbon Engineering Ltd., has developed an air-to-fuel technique to capture CO_2 directly from the atmosphere [10]. Electricity generated from RES has been used to split hydrogen from water. In the next step, hydrogen reacts with captured CO_2 to produce hydrocarbon fuels like diesel, and the entire process emits very little pollutants into the atmosphere. RES are unpredictable and intermittent. The availability of RES depends upon the local weather conditions of the selected location. Electricity generation from RES can be used in combination with grid supply or as a stand-alone system. In the case of stand-alone systems, hybrid energy-generating plants are economically feasible compared to systems using a single energy source [11]. This is because hybrid systems are less costly in electricity production, and the risk of power shortage is reduced compared to a single energy source. It was forecasted in 2015 by the Fraunhofer Institute for Solar Energy Systems that the capacity of solar PV may exceed 30TW peak power by 2050 [12]. Wind farms are now connected to the grid, and the electricity generation from wind turbines is available in the range of megawatts [13].

An important component in hybrid energy plants is the provision for storage of excess generated electricity. This excess electricity can be stored in the form of— (1) electrochemical energy (battery bank), (2) chemical energy (hydrogen), and (3) electrical energy (supercapacitors) [14]. Battery bank maintains power quality and provides short-term energy storage because of the self-discharge problem [15]. Hydrogen provides long-term storage (in months & years) for high volumes (in terawatt-hours) [16]. The improvement in electrolysers & their related components and the decrease in the cost of solar PV & wind technology are the main factors for motivating the concept of a 'hydrogen economy' [17]. As a result, hydrogen technology has been adopted by Japan, South Korea, China, and Germany [18].

India has taken the initiative of the National Green Hydrogen Mission to become a major exporter of hydrogen, with an incentive plan of $2.11 billion. This initiative is Strategic Interventions for Green Hydrogen Transition Programme (SIGHT) [19]. Under SIGHT, two distinct mechanisms exist: (1) to manufacture electrolysers with a 60 to 100 GW capacity in India and (2) to produce green hydrogen. The regions capable of producing/utilizing large-scale hydrogen will be developed as Green Hydrogen Hubs. The SIGHT program has three phases—(1) to establish policies and guidelines and initiate pilot projects (2022–2024), (2) to bring down manufacturing costs & promote incentives for large-scale production, to scale up production of green hydrogen (2025–2026), and (3) to focus on other distinctive hydrogen applications [19].

Hydrogen energy is the upcoming renewable energy system used in hybrid power plants to store excess electrical energy from the grid or RES. It has gained popularity because of the advancement in fuel cell technology [20]. Generally, a hydrogen energy system consists of three main apparatus for three process steps required for hydrogen production—(1) an electrolyser is required for producing hydrogen from the excess electricity generated from RES, (2) the hydrogen produced from step 1 is stored in a storage tank, and (3) the electricity is reproduced from stored hydrogen using a fuel cell [21]. During the process of production and reproduction of hydrogen, no pollutants are released into the atmosphere. Furthermore, hydrogen energy systems are efficient as the stored hydrogen does not degrade with time, and it attracts low maintenance costs for storing hydrogen for a considerably long time [22].

It is imperative to design the optimum size of the hybrid plant so that system components are fully utilized with minimum investment. This mainly depends on—(1) the availability of RES, (2) load demand, and (3) the weather conditions of the site [23]. To achieve the optimum system reliability and cost, one or a combination of different sizing methods like the graphical construction method, iterative method and artificial intelligence

method can be applied [24]. Some work has been done in many parts of the world to either reduce the cost of energy or provide electricity to places remotely located from the primary grid, along with the production of hydrogen [25]. Iran, China, Ecuadorian Amazon, Turkey, Egypt, UAE, Iraq, Afghanistan, and the USA have been these countries. Table 1 summarizes a study in these countries for hybrid energy plants prioritizing hydrogen production at various locations.

Table 1. Summary of different hybrid energy plants prioritizing hydrogen production.

Hybrid Plant Design	Study Location	On-Grid/ Off-Grid	COE ($/kWh)	Ref.
PV/HK/FC/Battery/HT/EL	Ecuadorian Amazon	Off-grid	0.184	[26]
PV/WT/HK	Iran	Off-grid	0.1155	[27]
SOFC-WGS-TSA-PEMFC	China	Off-grid	0.0395 to 0.0405	[28]
PV	Turkey	Off-grid	0.6124	[29]
PV/WT	Egypt	Off-grid	0.137 to 0.219	[30]
PV/FC	UAE	Off-grid	0.145	[31]
PV/FC	Iraq	Off-grid	0.195	[32]
PV/WT/BGG	Iran	Off-grid	0.128 to 0.223	[33]
PV/WT/BGG/FC	Iran	Off-grid	0.164 to 0.233	[34]
		On-grid	0.096 to 0.125	
PV/BM	China	Off-grid	0.6137	[35]
WT	Afghanistan	Off-grid	0.063 to 0.079	[36]
PV/WT/HK	Iran	Off-grid	0.1155	[37]
PV	Turkey	Off-grid	0.6124	[38]
WT	Afghanistan	Off-grid	0.0529 to 0.1135	[39]
PV/WT/battery/EL	USA	Off-grid	0.5	[1]

Legends: PV—photovoltaic, HK—hydro kinetic, FC—fuel cell, HT—hydrogen tank, EL—electrolyser, WT—wind turbine, SOFC—solid oxide fuel cell, WGS—water gas shift reaction, TSA—thermal swing adsorption, PEMFC—proton exchange membrane fuel cell, BGG—biogas generator, BM—bio mass.

This study has been conducted at SRM IST, Delhi NCR educational campus. A hybrid energy generating system (HEGS) has been proposed for meeting the load of 15 classrooms in an academic building. The geographical location of this campus has been marked in Figure 1 as 28.8377° north and 77.5826° east [40]. This area experiences approximately 300 solar days. During the winter season, it experiences minimum temperature reaches around 1 °C for 3 to 4 days. The data for average monthly solar radiation (ALLSKY INSOL), clearness index, diffuse horizontal irradiance (DIFF), direct normal radiance (DNR), average monthly temperature and average daylight hours for the Delhi-NCR region has been taken from NASA (National Aeronautics and Space Administration)—PDAV (Power Data Access Viewer) tool [41]. Figure 2 presents the ALLSKY INSOL & clearness index, and Figure 3 compares the selected region's ALLSKY INSOL, DIFF & DNR. DIFF is the light scattered at the earth's surface due to dust particles and moisture content in the atmosphere [42]. DNR is location specific and measured at the earth's surface, but it does not include the scattered radiation due to atmospheric components [43]. The average monthly temperature and daylight hours for this region are shown in Figure 4. The proposed HEGS has been analyzed for both on-grid and off-grid operations. Time series analysis and sensitivity analysis have been performed to validate the energy balance and to understand the impact of variation in the size of solar PV array, number of battery strings, reformer capacity & hydrogen tank capacity on NPC, renewable fraction, and CO_2 emissions.

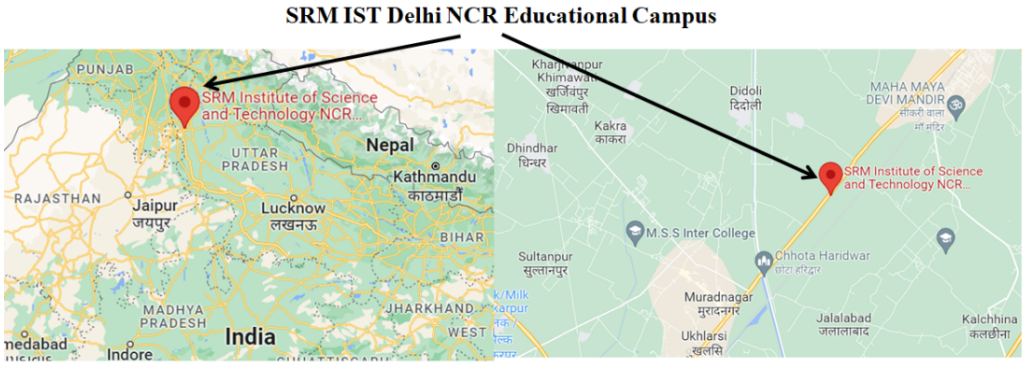

Figure 1. Map showing the location of SRM IST, Delhi-NCR Educational Campus.

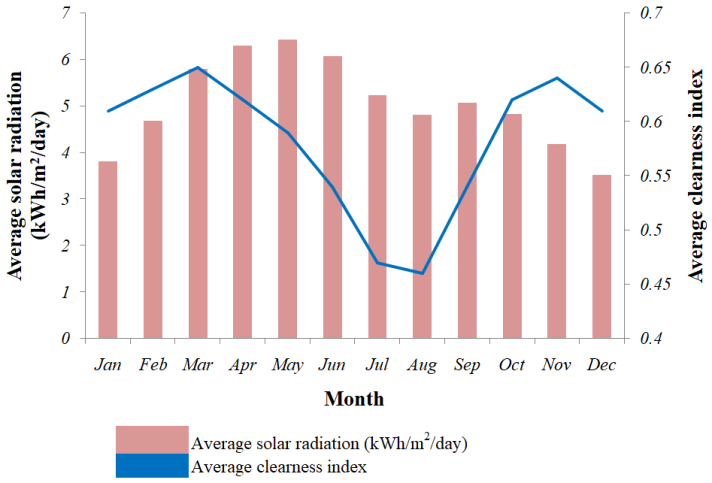

Figure 2. ALLSKY INSOL & clearness index of the selected region.

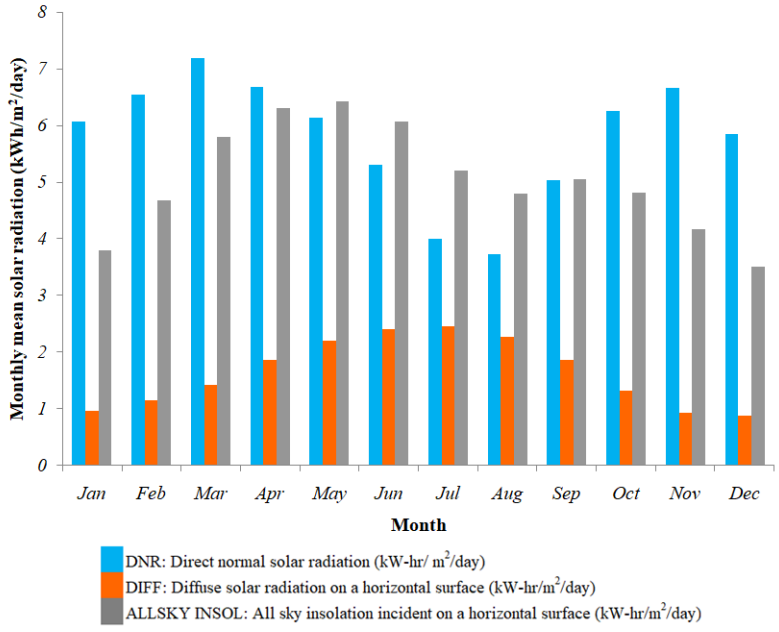

Figure 3. Comparison of ALLSKY INSOL, DIFF and DNR of the sun's radiation of the selected region.

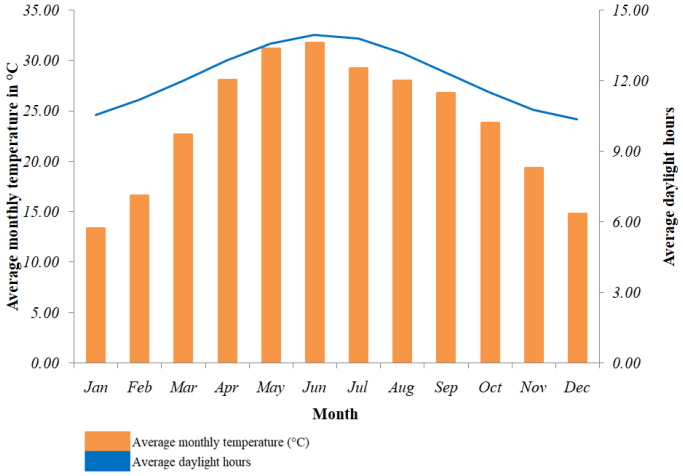

Figure 4. Average monthly temperature and daylight hours of the selected region.

The organization of the paper is as follows: in Section 1, the introduction and previous related work are discussed; the components of HEGS are discussed in Section 2; the sizing and economics of HEGS are discussed in Section 3; Section 4 provides the results and discussions; sensitivity analysis is provided in Section 5, and in Section 6, the conclusion is drawn.

2. The Hybrid Energy Generating System (HEGS)

A general model of renewable HEGS has been shown in Figure 5. In this model, solar energy is captured to generate electricity and hydrogen, which can be stored and utilized to serve the load as the dispatch strategy decides. The electrical energy can be stored in a battery bank, and hydrogen can be stored in a hydrogen tank. Hydrogen provides long-term energy storage; it has a high capacity but a low delivery rate. Therefore, to meet the short-span surges in load demand, it is required to have short-term storage of electricity as provided by the battery bank. It has a low capacity but a high delivery rate.

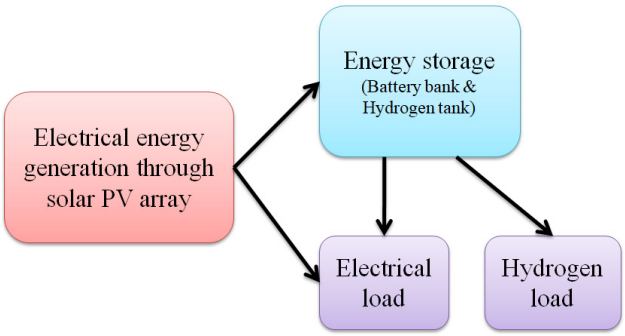

Figure 5. Renewable HEGS general model.

To serve the selected load, the proposed HEGS modelled in HOMER software has been shown in Figure 6. This HEGS consist of the following components—(1) solar PV array, (2) diesel generator (DG), (3) battery bank (BT), (4) electrolyser (ETL), (5) reformer (RFM), (6) hydrogen tank (HT), and (7) Grid. While choosing HEGS components, it is imperative to understand that oversizing the system will be expensive, while an under-sized system will fail to meet the load demand. Therefore, the simulation of the HEGS model has been done in HOMER software to minimize net present cost (NPC) for 24 h uninterrupted supply to load. The system with minimum NPC will also have a minimum cost of energy (COE). The constraints considered during the simulation were—(1) the 80% derating factor of the PV array, (2) the minimum load ratio of DG is 25%, (3) the state of charge (SOC) of the battery

is from 20% to 100%, (4) annual purchase capacity of the grid is 100 kW, (5) HEGS will not purchase electricity from grid between 9 AM to 4 PM and (6) HEGS lifetime is 25 years.

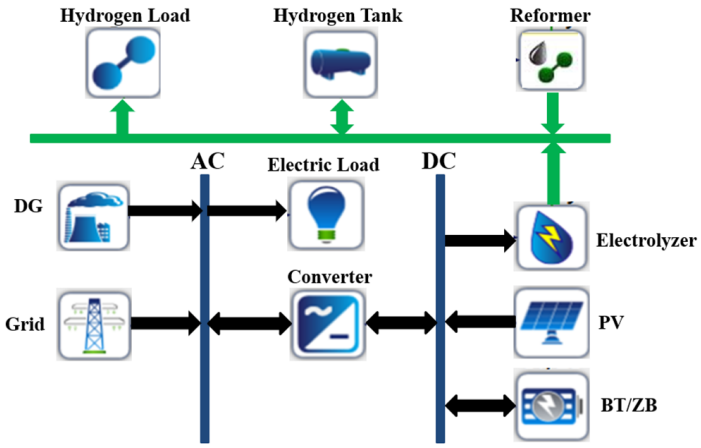

Figure 6. Modelling of proposed HEGS.

2.1. Energy Generation

The solar energy is captured by a PV array and converted to electrical energy. The size of the solar PV array is decided by the desired output voltage and current. The generic plat-plate PV module has been used to model the proposed HEGS. Suppose Y_{PV} is solar array output power from in kW. In that case, f_{PV} is the solar array derating factor in %, G_T is the solar radiation incident on the solar array in kW/m^2, $G_{T,STC}$ (1 kW/m^2) is the incident radiation from the sun, α_P is the power temperature coefficient in % per °C, T_c is the PV cell temperature in the current time step in °C, $T_{c,STC}$ is PV cell temperature under standard conditions (25 °C), then PV array power output, P_{output}, has been calculated using (1) [44]—the technical details solar PV array has been given in Table A1 in Appendix A.

$$P_{output} = Y_{pv} f_{pv} \left(\frac{G_T}{G_{T,STC}} \right) [1 + \alpha_p (T_c - T_{c,STC})] \quad (1)$$

When the electricity generated from the PV array and the energy stored in the battery bank cannot meet the load demand, a diesel-based generator operates to fulfil that deficiency. The fuel consumed by DG depends on the electricity generated. If F_0 is the coefficient of fuel curve intercept in L/h/kW, F_1 is the fuel curve slope in L/h/kW, Y_{gen} is the generator-rated capacity in kW, and P_{gen} is the generator power output in kW. Fuel consumed by DG, F, has been calculated using (2) [45].

$$F = F_0 Y_{gen} + F_1 P_{gen} \quad (2)$$

HOMER software has plotted the fuel curve for 50 kW DG with a slope of 0.333 L/h/kW and an intercept coefficient of 2.5 L/h, as shown in Figure 7. To fit the line to the data points, HOMER uses the linear least-squares method. The fuel consumption during the idle state is represented by the y-axis intercept, known as no-load fuel consumption. The slope of this curve is called marginal fuel consumption. If ρ_{DG} is the density of the diesel in kg/m^3, HLD is the lower heating response of the diesel in MJ/kg, and then the efficiency has been calculated using (3) [46]. The efficiency curve has been plotted from zero to rated output, as shown in Figure 8. The technical details DG has been given in Table A1 in Appendix A.

$$\eta_{DG} = \frac{3.6 P_{gen}}{F \rho_{DG} H_{LD}} \quad (3)$$

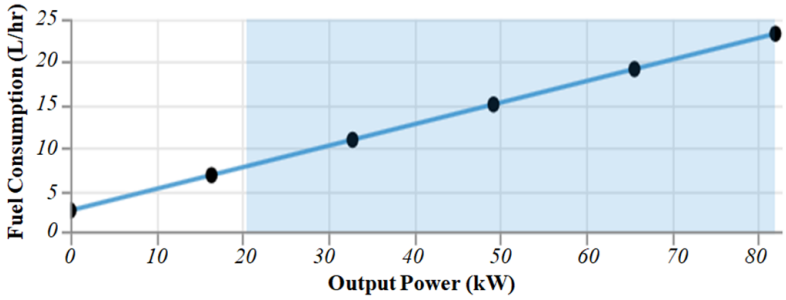

Figure 7. DG fuel curve.

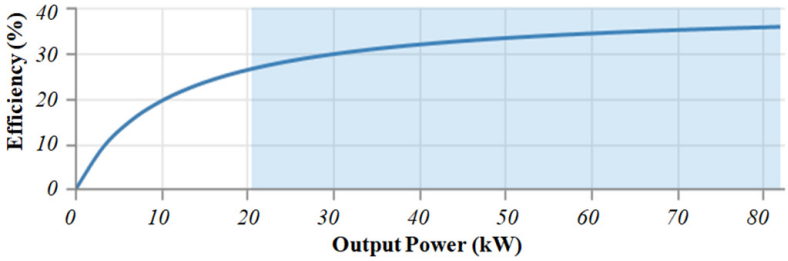

Figure 8. DG efficiency curve.

On connecting to the grid, the reliability of HEGS is enhanced. The electrical energy is generated mainly from the PV array. The excess energy is utilized in two ways—(1) it is stored in a battery bank to serve the load with the PV array during peak hours, and (2) to operate the electrolyser to produce hydrogen. DG is operated if electricity supplied by the PV array and battery bank is insufficient to serve the load. If the PV array, battery bank, and DG cannot serve the load, energy is purchased from the grid. The energy purchase and sell-back prices have been taken as $0.084 per kWh [47]. This price has been taken the same for all weekdays. Grid pollutant emissions per kWh are estimated to be 632 g of CO_2, 2.74 g of SO_2 and 1.34 g of NOx.

2.2. Energy Conversion

Hydrogen is produced by water electrolysis using electricity generated from HEGS. This hydrogen can be stored in a hydrogen tank for supplying to hydrogen load. Electrolyser efficiency is the ratio of the energy content (higher heating value) of the hydrogen produced to the amount of electricity consumed. Simply put, it is the efficiency of electrolysers converting electricity into hydrogen. The electrolyser efficiency ranges from 90% to 95%, and the hydrogen purity ranges from 99.8% to 99.9998% [48]. If N is the number of cells in the stack, Vt is the thermo-neutral voltage in V, Pi is the total input power to the stack in W, and I is the input current through the cell in A, the energy efficiency of the electrolyser, η_E, cell can be calculated as (4) [49].

$$\eta_E = \frac{NV_tI}{P_i} \quad (4)$$

A natural gas-based reformer is used to produce hydrogen. Natural gas contains methane, which produces hydrogen after undergoing thermal processes like a steam-methane reformation. In steam reforming, high-temperature steam (700–1000 °C) reacts with methane. This reaction produces hydrogen carbon monoxide and a very small amount of CO_2. The steam-methane reaction is shown in (5) [50]. In the final step, known as pressure-swing adsorption, pure hydrogen is obtained by removing CO_2 and other impurities.

$$CH_4 + H_2O(+\text{heat}) \rightarrow CO + 3H_2 \quad (5)$$

2.3. Energy Storage

After serving the electrical and hydrogen loads, the excess electricity generated can be stored in a battery bank. Whenever the PV array, DG or grid cannot meet the load demand, the electrical energy stored in the battery bank can be utilized to serve the load. Moreover, it helps to increase the renewable fraction by turning off DG during the daytime or lowering energy purchases from the grid. As the battery bank ensures an uninterrupted power supply to load, it becomes imperative to monitor battery SOC. It protects the battery from overcharging and goes beyond the minimum SOC required, adversely affecting the life of the battery. If Q(t) is the current capacity and Q(n) is the nominal capacity, then battery SOC can be calculated as provided in (6) [51].

$$\mathrm{SOC(t)} = \frac{\mathrm{Q(t)}}{\mathrm{Q(n)}} \tag{6}$$

If no loss of energy is assumed during the charging and discharging of the battery, the SOC related to the battery current is calculated as provided in (7) [1].

$$\mathrm{SOC(t)} = \mathrm{SOC(0)} + \frac{1}{\mathrm{C}} \int_0^{\mathrm{t}} \mathrm{I} \cdot \left(\mathrm{V_{BT}}, \mathrm{t}'\right) \cdot \mathrm{dt}' \tag{7}$$

C is the capacity of the battery in kWh, I is the battery current in A, and V_{BT} is the battery voltage in V.

The life of the battery depends upon two independent factors—(1) lifetime productivity and (2) float life of storage. For example, if suppose N_{BT} is the number of batteries in a battery bank. In that case, Q_{LP} is single battery lifetime productivity in kWh, Q_{SP} is annual storage productivity in kWh/year, and $L_{BT,f}$ is storage float life in years. Then, the life of the battery bank (L_{BT}) can be calculated using (8) [23]. The technical details battery bank is given in Table A1 in Appendix A.

$$\mathrm{L_{BT}} = \begin{cases} \frac{\mathrm{N_{BT}\ Q_{LP}}}{\mathrm{Q_{SP}}} \text{ If limited by productivity} \\ \mathrm{L_{BT,\,f}} \text{ If limited by lifetime} \\ \mathrm{MIN}\left(\frac{\mathrm{N_{BT}\ Q_{LP}}}{\mathrm{Q_{SP}}},\ \mathrm{L_{BT,\,f}}\right) \text{ If limited by productivity and lifetime} \end{cases} \tag{8}$$

The storage of hydrogen can be considered in a similar way to that of a battery. Depending upon the hydrogen tank capacity, the hydrogen is taken in ("charging phenomena") and delivered ("discharging phenomena") to the hydrogen load. As battery SOC has expressed in (7), the state of hydrogen (SOH) can be expressed as given in (9) [1].

$$\mathrm{SOH(t)} = \mathrm{SOH(0)} + \frac{1}{\mathrm{C_H}} \int_0^{\mathrm{t}} \dot{\mathrm{H}}_{\mathrm{m}} \left(\mathrm{P_H},\ \mathrm{t}'\right) \cdot \mathrm{d\ t}' \tag{9}$$

where C_H is the gravimetric capacity of the hydrogen storage tank in kg, $\dot{H}_m$ is the hydrogen mass flow rate in kg/h, and P_H is the hydrogen pressure.

Battery storage has lower power capital cost and higher round-trip efficiency, whereas hydrogen storage has lower capital energy cost and longer storage duration.

Comparison of Battery Technologies

A cost comparison of five types of battery technologies has been made in Table 2. Lead-acid (LA) and lithium-ion (LI) batteries are popularly used in HEGS to store excess energy produced. Recently, advanced battery technologies like vanadium flow (VF) and zinc bromide (ZB) flow batteries are replacing LA and LI batteries. This is mainly because the life of flow batteries is not compromised even if the batteries are not charged for a long time. Moreover, flow batteries provide higher energy capacity than LA and LI batteries. Because of its high robustness, long durability and tolerance against high temperatures,

nickel-iron (NI) is also becoming popular in HEGS for storing energy [52]. The annual SOC status of different battery technologies has been provided in Figure 9.

Table 2. Financial metrics of different battery technologies.

Battery Technology	Capital Cost ($ per kWh)	Replacement Cost ($ per kWh)	O&M Cost ($)	Life Span (Years)
LA battery	135	108	1.33 per year	5
LI battery	500	455	0	10
VF battery	535	465	0	25
ZB battery	800	735	0	25
NI battery	106	98	2.12	25

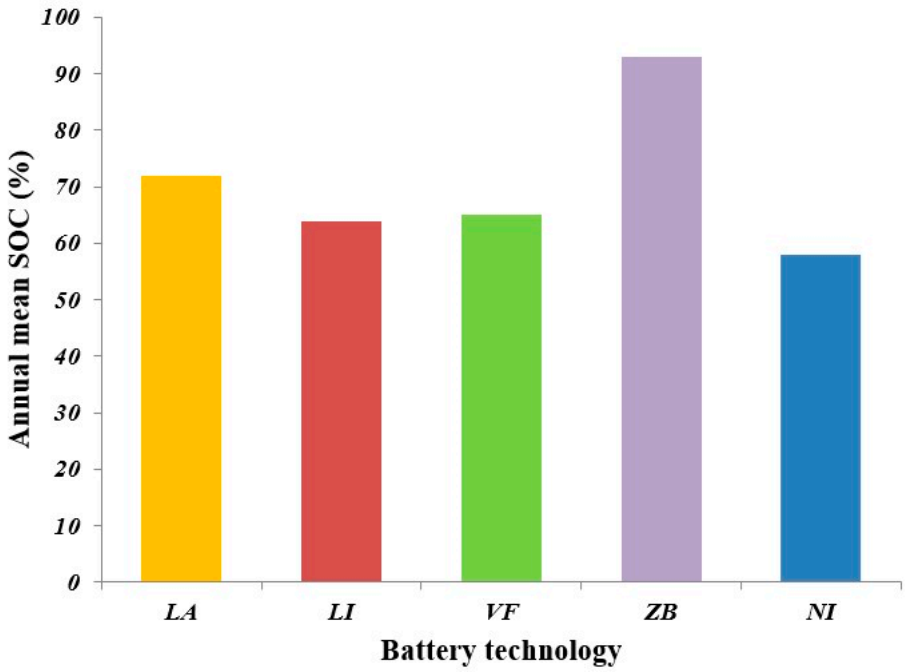

Figure 9. Annual mean SOC of different battery technologies.

3. Sizing and Economics of HEGS Components

For the effective function of HEGS, it is important to select the optimal sizing of the components to serve the energy demand of the selected load. This helps to achieve minimum COE after simulation. A number of optimal results are obtained after simulation, and different configurations of HEGS are expected to serve the load under consideration. The optimal solution is chosen based on optimum COE, NPC, and renewable fraction above 95% in HEGS.

3.1. Electric Load Demand Estimation

An academic building at SRM IST, Delhi-NCR campus, with 15 classrooms, has been considered a load. The details of the estimated load have been provided in Table 3. The load of one classroom consists of 6 LED lights, five ceiling fans, two air-conditioners, 1 LCD projector, 1 PA system (including microphone & speaker), one computer system and two plug points. The average electricity consumption of one classroom is estimated to be 26.58 kWh per day, and for 15 classrooms, it is approximately 400 kWh per day. The 24-h load profile and the yearly load profile have been presented in Figure 10a and 10b, respectively.

Table 3. Load estimation of 15 classrooms at SRM IST Delhi NCR campus.

Sr. No.	Load	Power (kW)	Quantity (Nos.)	Usage (h)	Total Load (kWh/Day)
1	LED light	0.024	6	6	0.864
2	Ceiling fans	0.020	5	6	0.6
3	Air conditioner (1.5 ton)	1.5	2	6	18
4	LCD Projector	0.28	1	6	1.680
5	PA system (microphone & speakers)	0.8	1	6	4.800
6	Computer system	0.1	1	6	0.6
7	Mobile charging point	0.003	2	6	0.036
The total load for one classroom					26.58
The total load for 15 classrooms					398.7 (~400)

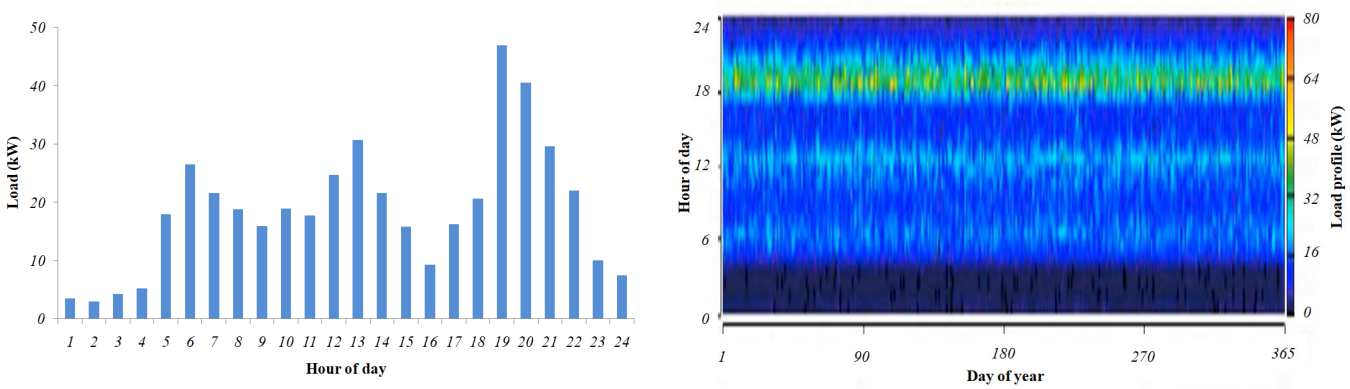

(**a**) (**b**)

Figure 10. (**a**) 24-h load profile and (**b**) yearly load profile of 15 classrooms at SRM IST Delhi-NCR campus.

3.2. HOMER Pro Software

Different software is available for finding the optimal HEGS configuration, like Hybrid2, RAPSim, and HYBRIDS. All these software is easy to use to provide long-term forecasts of HEGS performance. But the mentioned software does not offer economic analyses. On the other hand, hybrid Optimization of Multiple Electric Renewables (HOMER) software provides technical and economic analyses of HEGS [15].

In this study, the analysis has been done using HOMER software, which is developed by National Renewable Energy Laboratory, Golden, CO, USA. HOMER uses two optimization algorithms—the original grid search algorithm and the HOMER optimizer, to perform simulations. The optimized solutions are chosen based on the lowest NPC and lowest COE. Furthermore, the HOMER optimizer takes care of the maximum number of simulations per optimization, so the optimization process converges after a finite number of simulations.

It can be referred from Figure 11 that the geographical position of the selected location, weather conditions of the selected site, technical details of the components of the proposed HEGS and the load profile are the inputs to HOMER. Based on these inputs, the software performs simulations to obtain the optimal solutions. The outputs obtained from HOMER are the technical & economic data, number of estimated pollutants and sensitivity analysis, also known as what-if analysis, to understand the impact of one parameter on the other. The detailed flow chart of HOMER software has been provided as Figure A1 in Appendix B.

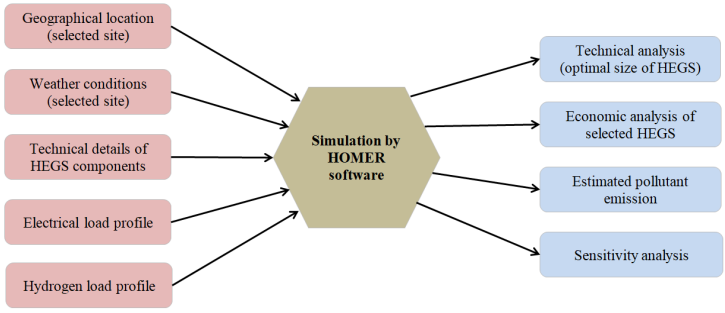

Figure 11. Block diagram process of HOMER software.

3.3. Cost Estimation of HEGS

The simulations performed by HOMER software can provide the optimal size of HEGS components to minimize the probability of loss of electricity supply and also minimize the NPC & COE. The HOMER performs technical and economic analysis by assuming that the cost of HEGS components increases at the same rate. The parameters considered to perform the calculation are annual interest rate, annual inflation rate and project lifetime. NPC is the summation of initial cost, replacement cost, cost of operation & maintenance (O&M), and cost of fuel, and from this, salvage value is subtracted. HOMER has used (10) to calculate NPC [53].

$$NPC = \sum_{N=1}^{t} r_d (C_{ini} + C_{rep} + C_{O\&M} + C_{fuel} - C_{sal}) \quad (10)$$

where, r_d (%) is the discount rate, N (years) is the project lifetime, C_{ini} ($) is the initial cost of the HEGS component, C_{rep} ($) is the replacement cost, $C_{O\&M}$ ($) is the operation and maintenance cost, C_{fuel} ($) is the fuel cost and C_{sal} ($) is the salvage value. If r is the annual interest rate, the discount rate can be calculated from (11) [54].

$$r_d = \frac{1}{(1+r)^N} \quad (11)$$

If r^o is the annual interest rate and f is the annual inflation rate, then the real annual interest rate, r, can be calculated from (12) [54].

$$r = \frac{r^0 - f}{1+f} \quad (12)$$

HOMER calculates the annualized cost, C_{ann}, by multiplying NPC with the capital recovery factor (CRF), as shown in (13) [54].

$$C_{ann} = CRF(r, N) \times NPC \quad (13)$$

CRF is a ratio used to calculate the present value of annual cash flows. HOMER calculates CRF as given in (14) [55].

$$CRF(r, N) = \frac{r(1+r)^N}{(1+r)^N - 1} \quad (14)$$

If E_{served} is the total electrical load served, HOMER calculates the levelized cost of energy, as shown in (15) [52].

$$COE = \frac{C_{ann}}{E_{served}} \quad (15)$$

HOMER uses (16) to calculate the levelized cost of hydrogen (COH) [1].

$$\mathrm{COH} = \frac{C_{ann} + V_e(E_P + E_{G,sales})}{M_H} \quad (16)$$

where, V_e is the value of electricity, E_P is the primary electrical load, $E_{G,sales}$ is the total energy sold to the grid, and M_H is the total hydrogen production.

4. Results and Discussions

To perform simulation, HOMER takes the technical details of HEGS components, its initial cost, replacement cost, O&M cost, and lifespan of components as input. To calculate the economic parameters, discount rate, inflation rate and interest rate are also taken as input. The financial metrics provided as input to HOMER have been provided in Table 4. A total of 4607 solutions have been simulated by HOMER, out of which 48 feasible solutions have been obtained. Based on the selection criteria, four solutions have been selected for the analysis, which is presented in Section 4.1.

Table 4. Financial metrics of HEGS components.

Components	Initial Cost ($)	Replacement Cost ($)	O&M Cost ($)	Life Span
PV	$470 per kW	$470 per kW	$2.66 per year	25 years
DG	$665 per kW	$535 per kW	$0.027 per op. h	15,000 h
Converter	$195 per kW	$195 per kW	$4 per year	15 years
Battery	$800 per kWh	$735 per kWh	$10 per year	30 years
Electrolyser	$1500 per kW	$1500 per kW	$0.05 per year	20 years
Reformer	$3500 per kW	$3200 per kW	$200 per year	25 years
Hydrogen tank	$600 per kg	$600 per kg	$10 per year	25 years

Electricity generation from renewable sources is lowly reliable. This is due to uncertainty in weather conditions. In Figure 5, the renewable source of electricity generation is a solar PV array. The excess electricity generated from the PV array will charge the battery bank and be used by the electrolyser to generate hydrogen. In the proposed HEGS, DG serves as a captive power generation source when the PV array & battery bank cannot meet the load demand and the grid is under maintenance/repair work. Therefore, the inclusion of DG increases the reliability of HEGS. The composition of diesel has been 0.4% sulphur content, 88% carbon content, 43.2 MJ/kg of lower heating value and a density of 820 kg/m^3. Estimated emissions per litre of diesel consumption are 16.5 g of CO, 0.72 g of unburned hydrocarbon, 0.1 g of particulate matter and 15.5 g of NOx.

4.1. Optimization Results and Economic Analysis

The criteria for choosing the optimum solutions have been—(1) continuous supply of electricity to load, (2) optimum COE & NPC, (3) high value of the renewable fraction, and (4) low value of pollutant emission. Based on these criteria, four combinations have been chosen for the proposed HEGS—(1) PV/BT/Grid/ETL/RFM/HT (without DG), (2) PV/DG/BT/Grid/ETL/RFM/HT, (3) PV/DG/BT/ETL/RFM/HT (without Grid), and (4) PV/DG/Grid/ETL/RFM/HT (without battery). The simulation results for the proposed HEGS obtained from HOMER have been presented in Table 5. From a financial metrics point of view, comparisons have been made for COE ($/kWh), NPC ($), operating cost ($/year), initial cost ($), O&M cost ($/year), fuel cost ($/year). Combination 1 has the lowest NPC ($1,285,037) & least COE ($0.395 per kWh). The operating cost ($26,475 per year) is the lowest for combination 2. The lowest O&M cost ($21,955 per year) has been obtained for combination 3. The fuel cost ($107 per year) is the lowest for combinations 2 and 3. It can be observed from Table 5 that nominal battery capacity (7000 kWh) is the highest

in combination 3. This provides more storage of electrical energy compared to other combinations. The lowest battery storage capacity is found in combination 2 (1000 kWh), as the grid is connected here to take care of any shortfall while serving the load demand. The comparison of total system cost for the selected HEGS combinations has been shown in Figure 12. A comparison of COE and the cost of hydrogen is shown in Figure 13.

Table 5. Optimization results obtained for proposed HEGS (Part—I).

	Architecture										Financial Metrics					
HEGS Combination	PV (kW)	DG (kW)	Battery (No. of Strings)	Battery Nominal Capacity (kWh)	Grid (kW)	Electrolyser (kW)	Reformer (kW)	Hydrogen Tank (kg)	Converter (kW)	Dispatch Strategy	COE ($/kWh)	NPC ($)	Operating Cost ($/Year)	Initial Cost ($)	O&M Cost ($/Year)	Fuel Cost ($/Year)
1.	200		3	3000	100	100	100	100	38	CC	0.395	1,285,037	27,903	663,890	22,015	
2.	200	82	1	1000	100	100	100	100	40	LF	0.402	1,306,485	26,475	717,116	21,990	107
3.	200	82	7	7000		100	100	100	70	CC	0.408	1,327,521	26,942	727,756	21,955	107
4.	200	82			100	100	100	100	42	CC	0.444	1,442,017	32,584	716,655	28,692	2832

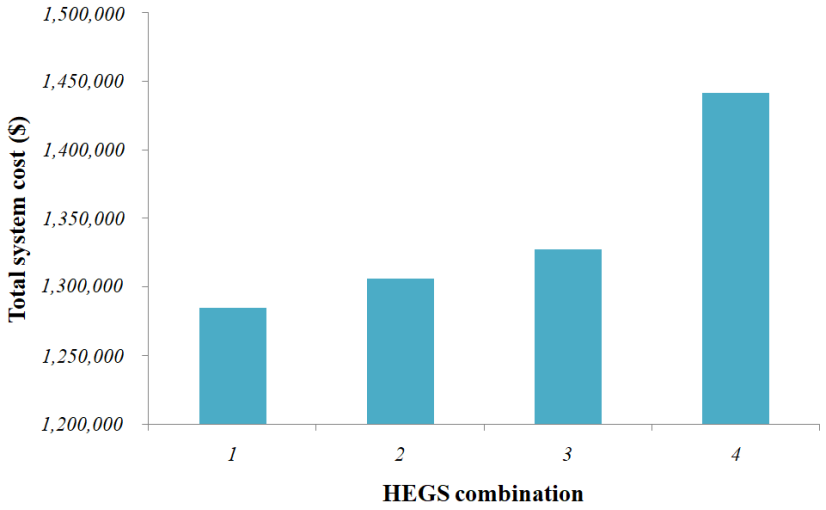

Figure 12. Comparison of total system cost for selected HEGS combination.

4.2. Technical Analysis

The summary of the technical report is provided in Table 6. From a technical point of view, combination 1, 3 & 4 follows the cycle charging (CC) dispatch strategy. In CC strategy, the DG or grid operates at full capacity to serve the load. The excess electricity produced in this case is utilized to charge the battery bank and serve the electrolyser. Combination 2 follows the load-following (LF) strategy. In the LF strategy, the DG or grid operates to generate enough electricity to meet the load demand. The battery bank is charged when a renewable source like a solar PV array generates electricity. The renewable fraction is found to be highest for combination 3, which is 99.8% and the lowest can be observed for combination 4, which is 44.2%. It has been estimated that in combination 4, energy purchased from the grid has been approximately 20% compared to 1% in the case

of combinations 1 & 2 and 0% in the case of combination 3. The usage of DG is highest in the case of combination 4 compared to other combinations. It is also observed that the percentage of excess electricity generation (17%) is highest in combination four among all other combinations. This may be due to the absence of a battery bank in combination 4, and DG is used as a compensator.

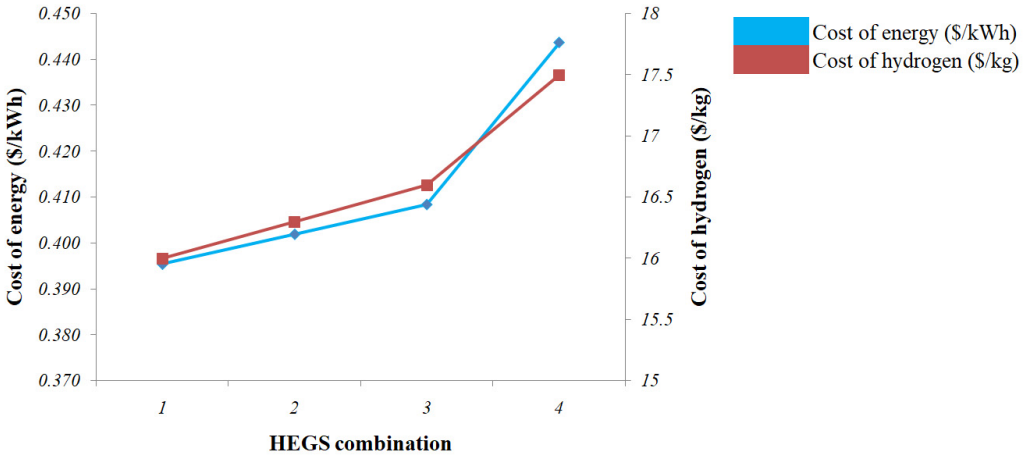

Figure 13. Comparison of cost of energy & cost of hydrogen for selected HEGS combination.

Table 6. Optimization results obtained for proposed HEGS (Part—II).

	Architecture											Electricity Generated (kWh/Year)				Grid	
HEGS Combination	PV (kW)	DG (kW)	Battery (No. of Strings)	Battery Nominal Capacity (kWh)	Grid (kW)	Electrolyser (kW)	Reformer (kW)	Hydrogen Tank (kg)	Converter (kW)	Dispatch Strategy	Renewable Fraction (%)	DG	PV	Excess Electricity Production (%)	Excess Electricity Production (kWh/Year)	Energy Purchased (kWh)	Energy Sold (kWh)
1.	200		3	3000	100	100	100	100	38	CC	97.7	0	296,363	3	9273	3285	0
2.	200	82	1	1000	100	100	100	100	40	LF	97.8	246	296,363	3	9255	2987	0
3.	200	82	7	7000		100	100	100	70	CC	99.8	246	296,363	3	9016	0	0
4.	200	82			100	100	100	100	42	CC	44.2	6533	296,363	17	62,542	74,976	0

The emission of CO_2 into the atmosphere is causing a planetary crisis. So, HEGS combination 3, which has a maximum renewable fraction (99.8%), has been selected as the optimal solution. This combination 3 provides a stand-alone solution for the proposed HEGS, which not only reduces the dependency on the grid but has no contribution towards CO_2 emissions from the grid. The absence of a grid in this combination has been compensated by increased battery nominal capacity (7000 kWh) compared to other HEGS combinations. The SOC of the battery bank is shown in Figure 14, and it is observed that for most days, SOC lies in the range of 80% to 100%. Therefore, the energy from the battery bank has mainly been used between the 0 to 11th hour and the 18th to 24th hours. Figure 15 shows the monthly average of electricity production from solar PV array and DG and the total electrical load served. The yearly power output from the solar PV array

and DG is shown in Appendix B in Figures A2 and A3, respectively. The input power taken by the electrolyser has been shown in Figure A4 in Appendix B. Figure 16 shows the monthly average of hydrogen production from the electrolyser and the reformer, along with the total hydrogen load served. The yearly hydrogen output from the reformer is shown in Figure A5, and the yearly status of the hydrogen tank level is shown in Figure A6 in Appendix B.

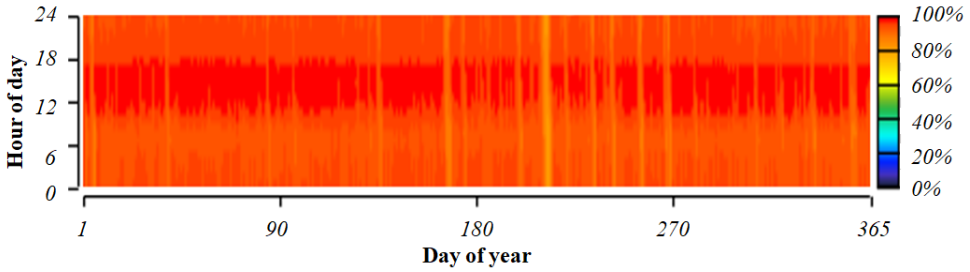

Figure 14. Yearly SOC status of battery bank of HEGS combination 3.

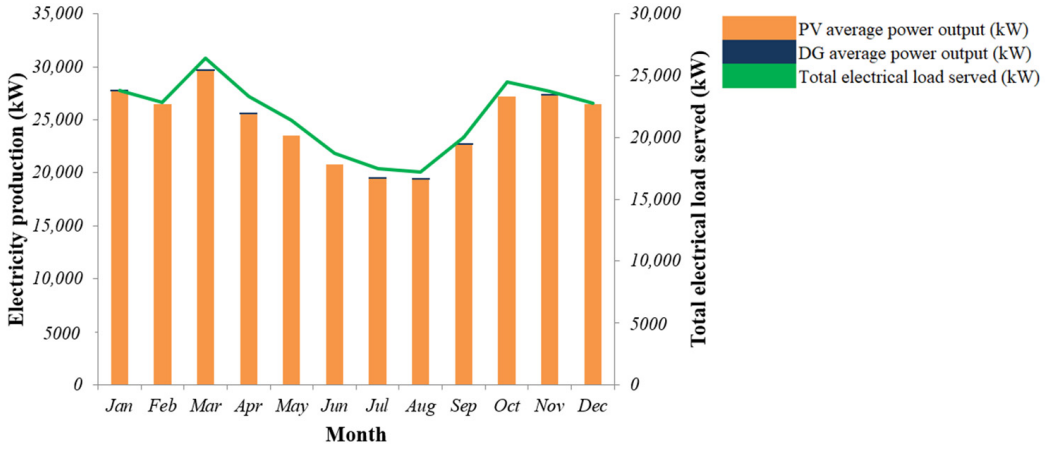

Figure 15. Monthly average electricity production by HEGS combination 3.

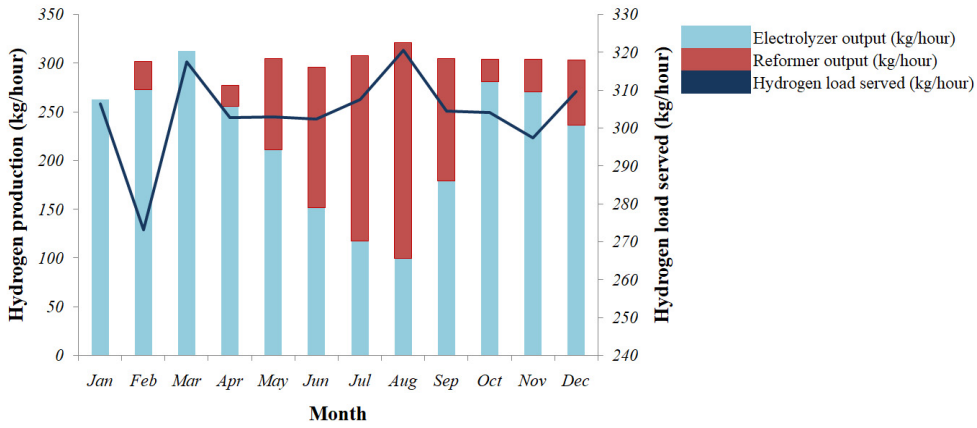

Figure 16. Monthly average hydrogen production by HEGS combination 3.

4.3. Time-Series Analysis

To check the energy balance for 24-h operation of combination 3 HEGS, a time-series analysis was done on the 2nd day of January. The electricity generators have been solar PV array & DG, while the battery charges after meeting the load demand and supplies electricity when needed. The electricity has been consumed by the AC load and the electrolyser. The contributions of all these mentioned HEGS components have been plotted in Figure 17. The observations from this plot have been provided in Table 7.

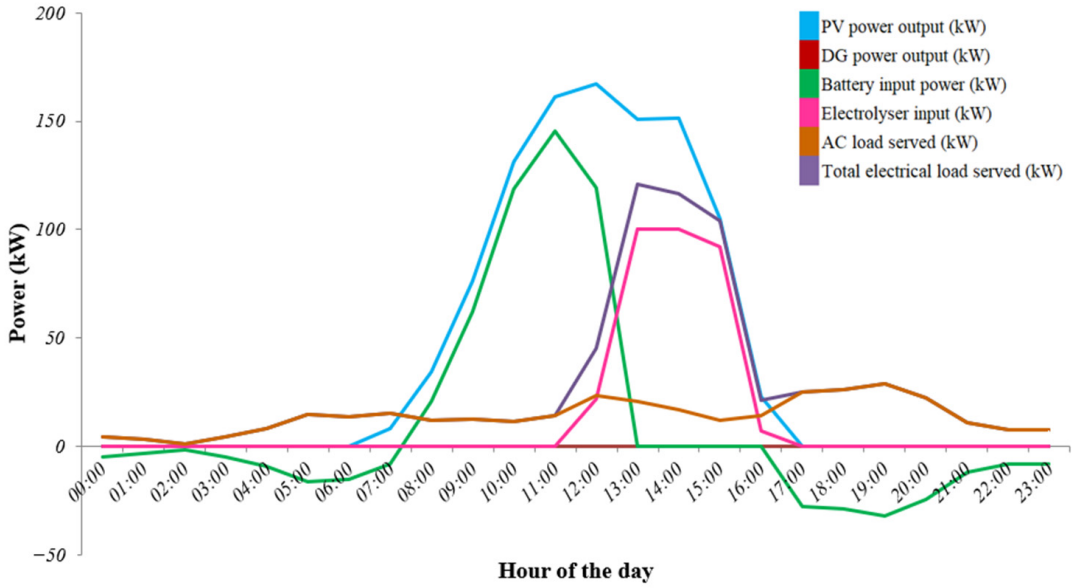

Figure 17. Time series analysis for 24 h operation of HEGS.

Table 7. Time series analysis for the 2nd day of January.

Time Duration	HEGS Component Contribution
0 to 6th hours	• Solar PV array has been unable to generate electricity without sunlight. • Energy served in the battery bank served the load.
6th to 17th hours	• Solar PV array generates electricity. • Battery bank charges till the 13th hour & it did not operate from the 13th to the 16th hour. It started to serve the load (along with the solar PV array) from the 16th hour. • The electrolyser consumed electricity from the 11th to 17th hour and AC primary load.
17th to 23rd hours	• As load demand reduces, it is met with energy stored in the battery bank

On this date, the DG was not required to be operated. The energy balance calculation, provided in Table 8, has been done for the 12th hour of the day. This validates that the total electricity generated equals the total consumed.

Table 8. Energy balance calculation from time series plot at 12th hour.

	HEGS Component	Power Generated/Consumed
Electricity generated	Solar PV array	A = 167 kW
	Diesel generator	B = 0 kW
Electricity served to load	Battery bank	C = 119 kW
Electricity consumed	Electrolyser	D = 21.86 kW
Inverter operation	Input power to the inverter	E (=A + B − C − D) =26.14 kW
	Output power to the inverter (Inverter efficiency = 90%)	F = 23.53 kW
Electricity consumed	AC load served	G = 23.53 kW (this value is equal to F)
	Total electrical load served	(=D + G) =45.39 kW

4.4. Pollutant Emissions

It is imperative to consider the pollutant emission before choosing an optimal solution for the proposed HEGS. The summary of pollutant emissions is provided in Table 9. The highest CO_2 emission has been observed from combination 4 (53,888 kg/year) and the lowest from combination 3 (247 kg/year). In HEGS combination 4, the energy is generated through a solar PV array, and if required, DG is operated to meet the load demand. In this combination, the battery bank is not a part of HEGS, so there is no provision for storing energy. On referring Table 6, it can be observed that DG has generated 6533 kWh per year of electricity, which is the highest value among all combinations. This means that DG has been operated a maximum number of times and consumed fuel worth $2832 annually. So, concerning emissions from DG, pollutant emission is highest in combination 4. In case of a shortfall of electricity generation from PV and DG, energy has to be purchased from the grid to fulfill the load demand. The grid generates electricity using fossil fuels, and hence, the emission of CO_2 is highest among the other HEGS combinations.

Table 9. Summary of pollutant emissions for proposed HEGS.

	Architecture											Emissions					
HEGS Combination	PV (kW)	DG (kW)	Battery (No. of Strings)	Battery Nominal Capacity (kWh)	Grid (kW)	Electrolyser (kW)	Reformer (kW)	Hydrogen Tank (kg)	Converter (kW)	Dispatch Strategy	Renewable Fraction (%)	CO_2 (kg/Year)	CO (kg/Year)	UHC (kg/Year)	PM (kg/Year)	SO_2 (kg/Year)	NOx (kg/Year)
1.	200		3	3000	100	100	100	100	38	CC	97.7	2076	0	0	0	0	4.4
2.	200	82	1	1000	100	100	100	100	40	LF	97.8	2134	1.55	0.0678	0.00942	8.68	5.46
3.	200	82	7	7000		100	100	100	70	CC	99.8	247	1.55	0.0678	0.00942	0.468	1.46
4.	200	82			100	100	100	100	42	CC	44.2	53,888	41	1.79	0.248	219	139

The grid is not a part of combination 3, so the emissions from grid operation have been avoided. It can also be observed from Table 9 that the nominal capacity of the battery bank (7000 kWh) is the highest among all combinations. So, this combination provides maximum provision for the storage of excess electricity. The DG has been operated least often, so CO_2 emissions are the lowest in this combination. Figure 18 presents the comparison of CO_2 emissions & renewable fractions for selected HEGS combinations.

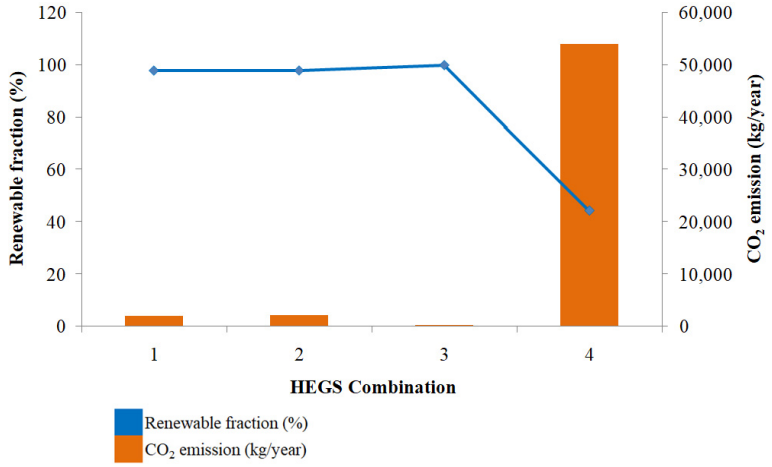

Figure 18. Comparison of CO_2 emissions & renewable fraction for selected HEGS combinations.

5. Sensitivity Analysis

A HEGS is a complex connection of different components. The optimum working of HEGS depends on different variables. Changes in some variables may bring huge changes in the working of HEGS. So, it is imperative to study the impact of such variables on the operation of HEGS. This what-if analysis is known as sensitivity analysis. The sensitivity analysis has been performed for combination 3. This combination has followed the CC dispatch strategy. The analysis has been performed between—(1) the size of the solar PV array and the number of battery strings and (2) the reformer and hydrogen tank capacity. The sensitivity variables are NPC, renewable fraction, and CO_2 emissions. The variation in COE has been marked in each of the analyses for a clear overview.

The optimization plot has been plotted between COE and renewable fraction, considering 25 years project lifetime. This plot is shown in Figure 19. The encircled points in the plot are the feasible solutions for that particular sensitivity case. It can be observed that many points lie in the region of high renewable fraction, which has the cost of energy between \$0.4 to 0.6 per kWh.

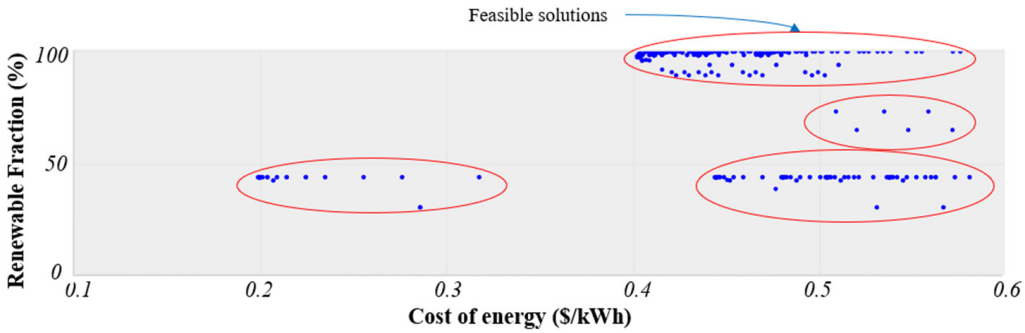

Figure 19. Optimization plot between COE and renewable fraction for 25 years project lifetime.

In Figure 20a, the impact of variation in NPC with COE values superimposed has been shown. The least COE has been obtained as \$0.408 per kWh for seven battery strings, 200 kW solar PV array, 82 kW DG, 100 kW ETL, 100 kW RFM, and 100 kg HT with NPC of \$1,327,521. In Figure 20b, the impact of variation in renewable fraction has been analyzed to understand the percentage of green energy production. It can be observed from this plot that the point of least COE lies within 90% to 100% of the renewable fraction. The impact of variation in CO_2 emissions has been shown in Figure 20c. It shows CO_2 emissions reductions in areas where the renewable fraction is above 90%. Figure 21 presents the impact of variation in NPC on the capacity reformer and hydrogen tank capacity.

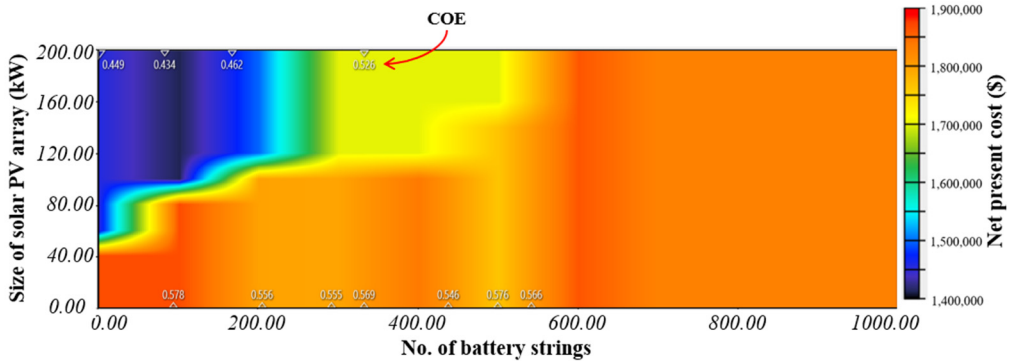

(**a**)

Figure 20. *Cont.*

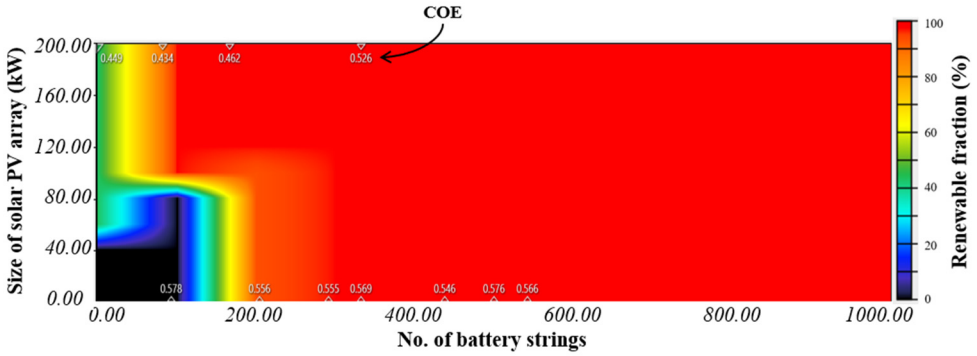

(**b**)

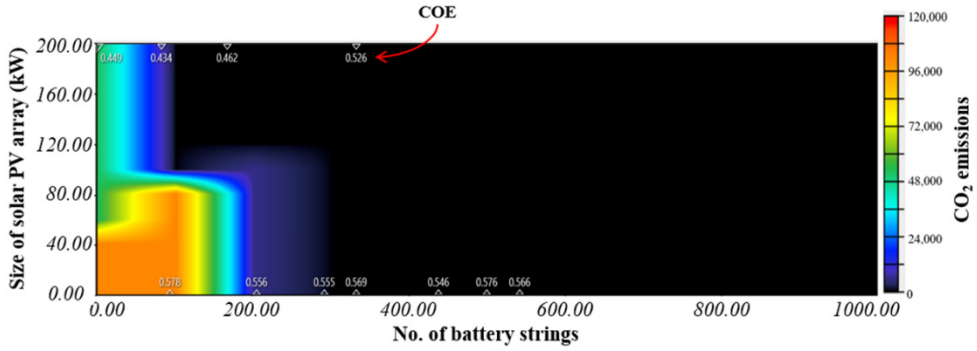

(**c**)

Figure 20. Sensitivity analysis between the size of solar PV array & number of battery strings with variation in (**a**) NPC, (**b**) renewable fraction, and (**c**) CO_2 emissions.

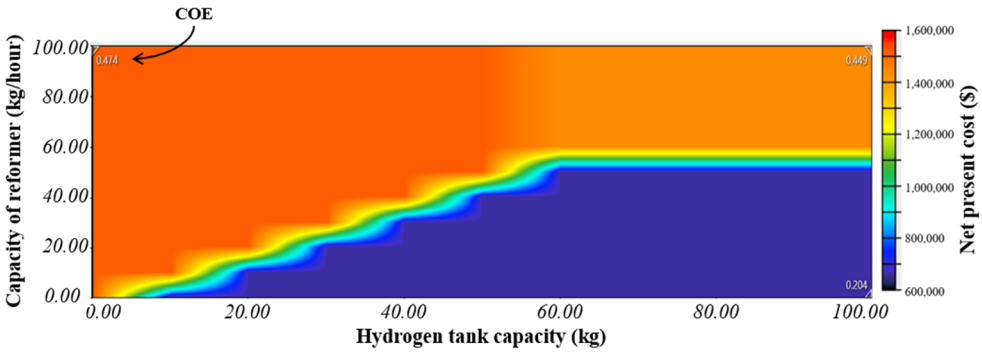

Figure 21. Sensitivity analysis for reformer and hydrogen tank capacity with variation in NPC.

6. Conclusions

In this study, the aim has been to compare the proposed HEGS solutions for on-grid and off-grid operations. The selected optimal solution has been taken as PV (200 kW)/DG (82 kW)/BT (7000 kWh) for electricity generation along with ETL (100 kW)/RFM (100 kW)/HT (100 kg) for green hydrogen production. The optimal solution has been chosen based on low O&M cost ($21,955 per year), a high renewable fraction (99.8%), and low CO_2 emissions (247 kg/year). The conclusions drawn from this work are mentioned below:

1. The electricity generation has been using 200 kW PV, 82 kW DG, 7000 kWh BT, and a converter of 70 kW, with a CC dispatch strategy.
2. The initial cost of HEGS has been estimated to be $727,756, and the operating cost is $26,942 per year.
3. The NPC has been estimated to be $1,327,521; the estimated COE will be $0.408 per kWh, and the cost of hydrogen will be $16.6 per kg.
4. The CO_2 emission will be reduced to 247 kg/year.

5. Sensitivity analysis has been performed in two parts—(a) the impact of variation in solar PV array size & number of battery strings has been studied with sensitivity variables such as NPC, renewable fraction & CO_2 emissions, and (b) the impact of variation in reformer capacity & hydrogen tank capacity, has been studied with NPC as sensitivity variable.

In future work, the government policies, subsidies provided by the government and tariffs regulated by the energy sector can be considered to improvise the analysis.

Author Contributions: Resources, G.F. and L.E.; Supervision, H.S. and V.B.; Writing—original draft, S.S.; Writing—review & editing, H.S., V.B. and P.K. All authors have read and agreed to the published version of the manuscript.

Funding: This research received no external funding.

Institutional Review Board Statement: Not applicable for studies not involving humans or animals.

Informed Consent Statement: Not applicable for studies not involving humans.

Data Availability Statement: The authors confirm that all data have been presented.

Conflicts of Interest: The authors declare no conflict of interest.

Appendix A

Table A1. Technical details of solar PV array, DG, and battery.

	Description	Value
Solar PV array	Type of panel	Flat plate
	Rated capacity (kWp)	1
	Capital cost ($/kW)	470
	Replacement cost ($/kW)	470
	O&M cost ($/year)	2.66
	Lifetime (years)	25
	Derating factor (%)	80
	Temperature coefficient (per °C)	−0.5
	Nominal operating cell temperature (°C)	47
	Efficiency (%)	0.13
Diesel generator	Fuel	Diesel
	Capital cost ($/kW)	665
	Replacement cost ($/kW)	535
	O&M cost ($/h)	0.027
	Fuel price ($/L)	1.14
	Lifetime (hours)	15,000
	CO (g/L/fuel)	16.5
	Unburned HC (g/L fuel)	0.72
	Particulates (g/L fuel)	0.1
	Fuel sulfur to PM (%)	2.2
	NOX (g/L fuel)	15.5
Battery	Nominal voltage (V)	600
	Nominal capacity (kWh)	1000
	Maximum capacity (Ah)	1670
	Round-trip efficiency (%)	90
	Maximum charge current (A)	1670
	Maximum discharge current (A)	5000

Appendix B

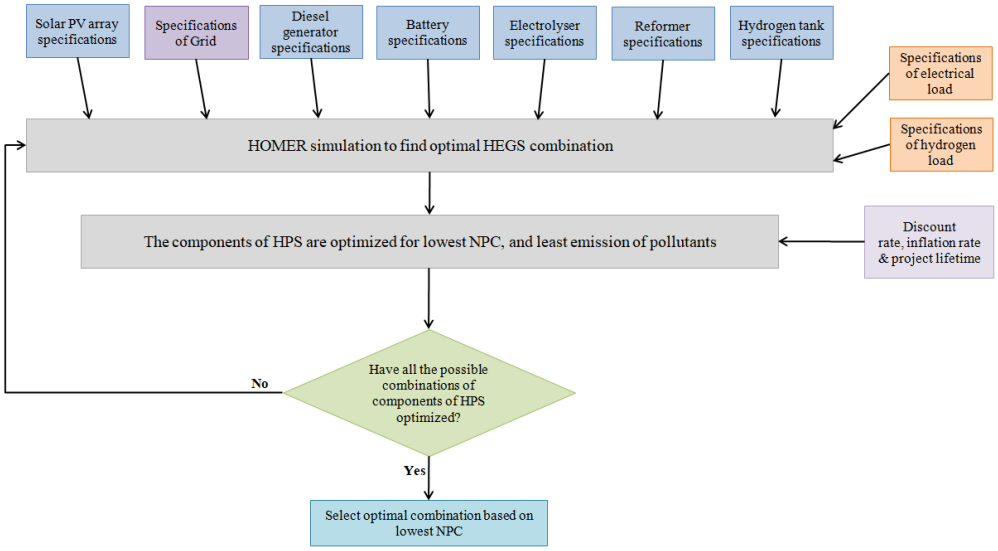

Figure A1. Flow chart of HOMER software.

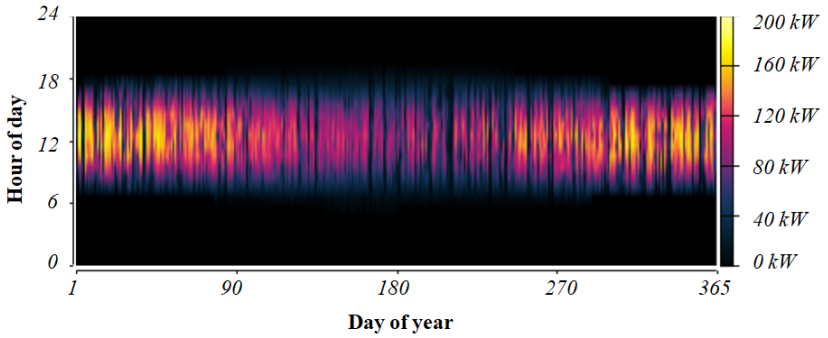

Figure A2. Power output from solar PV array in HEGS combination 3.

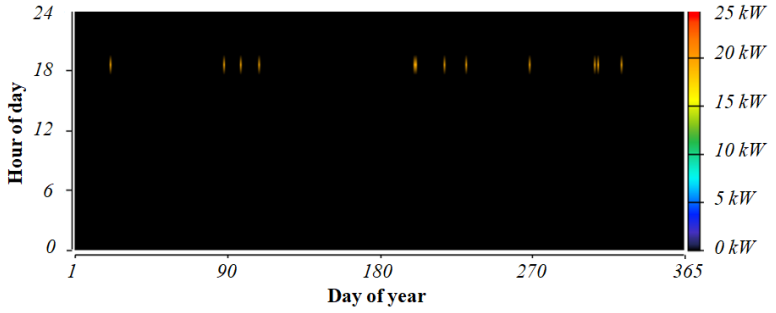

Figure A3. Power output from DG in HEGS combination 3.

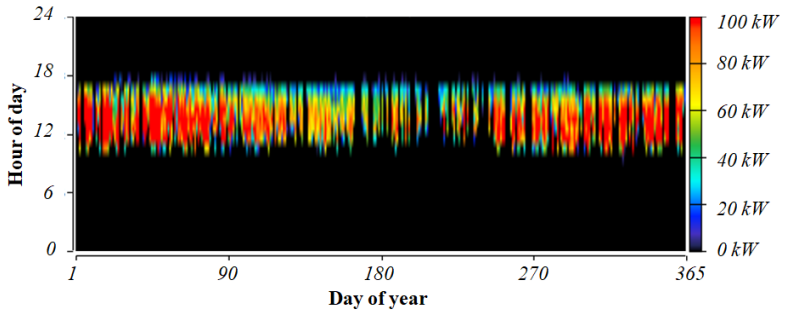

Figure A4. Electrolyser input power in HEGS combination 3.

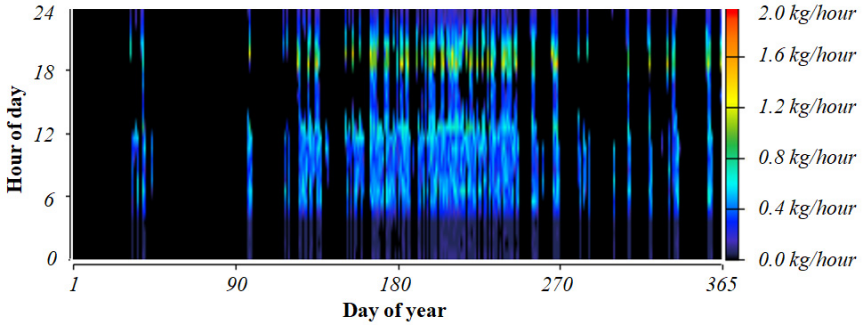

Figure A5. Hydrogen output from reformer in HEGS combination 3.

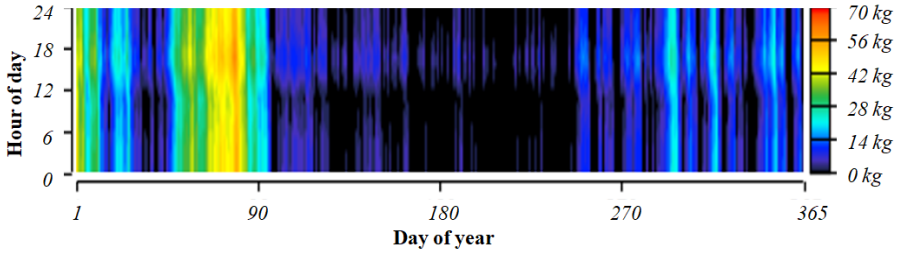

Figure A6. Hydrogen tank level in HEGS combination 3.

References

1. Abdin, Z.; Mérida, W. Hybrid energy systems for off-grid power supply and hydrogen production based on renewable energy: A techno-economic analysis. *Energy Convers. Manag.* **2019**, *196*, 1068–1079. [CrossRef]
2. Ekonomou, L.; Fotis, G.P.; Vita, V.; Mladenov, V. Distributed Generation Islanding Effect on Distribution Networks and End User Loads Using the Master-Slave Islanding Method. *J. Power Energy Eng.* **2016**, *4*, 1–24. [CrossRef]
3. Amini, A.; Abedi, M.; Nesari, E.; Daryadel, E.; Kolahi, M.; Mianabadi, H.; Fisher, J. The paris agreement's approach toward climate change loss and damage. *World Aff.* **2023**, *186*, 46–80. [CrossRef]
4. Shapiro, A.F.; Metcalf, G.E. The macroeconomic effects of a carbon tax to meet the U.S. Paris agreement target: The role of firm creation and technology adoption. *J. Public Econ.* **2023**, *218*, 104800. [CrossRef]
5. Sharma, H.; Pal, N.; Singh, Y.; Sadhu, P.K. Development and Simulation of Stand Alone Photovoltaic Model Using Matlab/Simulink. *Int. J. Power Electron. Drive Syst.* **2015**, *6*, 703. [CrossRef]
6. Hofrichter, A.; Rank, D.; Heberl, M.; Sterner, M. Determination of the optimal power ratio between electrolysis and renewable energy to investigate the effects on the hydrogen production costs. *Int. J. Hydrogen Energy* **2023**, *48*, 1651–1663. [CrossRef]
7. Fotis, G.; Dikeakos, C.; Zafeiropoulos, E.; Pappas, S.; Vita, V. Scalability and Replicability for Smart Grid Innovation Projects and the Improvement of Renewable Energy Sources Exploitation: The FLEXITRANSTORE Case. *Energies* **2022**, *15*, 4519. [CrossRef]
8. Peyvandi, M.; Hajinezhad, A.; Moosavian, S.F. Investigating the intensity of GHG emissions from electricity production in Iran using renewable sources. *Results Eng.* **2023**, *17*, 100819. [CrossRef]
9. Dogan, E.; Hodžić, S.; Šikić, T.F. Do energy and environmental taxes stimulate or inhibit renewable energy deployment in the European Union? *Renew. Energy* **2023**, *202*, 1138–1145. [CrossRef]
10. He, S.; Barati, B.; Hu, X.; Wang, S. Carbon migration of microalgae from cultivation towards biofuel production by hydrothermal technology: A review. *Fuel Process. Technol.* **2023**, *240*, 107563. [CrossRef]
11. Sambhi, S.; Sambhi, S.; Bhadoria, V.S. IoT based optimized and secured ecosystem for energy internet: The state of the art. In *Internet of Things in Business Transformation: Developing an Engineering and Business Strategy for Industry 5.0*; Scrivener Publishing LLC: Beverly, MA, USA, 2021; pp. 91–126. [CrossRef]
12. Mukhammadiev, M.M.; Urishev, B.U.; Uulu, A.A.; Almardanov, O.; Karimova, N.E.; Murodov, H. The role of renewable energy sources in providing the efficiency of the power system in the conditions of digital energy transformation. In *AIP Conference Proceedings*; AIP Publishing LLC: Melville, NY, USA, 2023; Volume 2552, p. 050019. [CrossRef]
13. Kreishan, M.Z.; Fotis, G.P.; Vita, V.; Ekonomou, L. Distributed Generation Islanding Effect on Distribution Networks and End User Loads Using the Load Sharing Islanding Method. *Energies* **2016**, *9*, 956. [CrossRef]
14. Adewumi, O.B.; Fotis, G.; Vita, V.; Nankoo, D.; Ekonomou, L. The Impact of Distributed Energy Storage on Distribution and Transmission Networks' Power Quality. *Appl. Sci.* **2022**, *12*, 6466. [CrossRef]
15. Sambhi, S.; Sharma, H.; Kumar, P.; Fotis, G.; Vita, V.; Ekonomou, L. Techno-Economic Optimization of an Off-Grid Hybrid Power Generation for SRM IST, Delhi-NCR Campus. *Energies* **2022**, *15*, 7880. [CrossRef]
16. Le, S.T.; Nguyen, T.N.; Linforth, S.; Ngo, T.D. Safety investigation of hydrogen energy storage systems using quantitative risk assessment. *Int. J. Hydrogen Energy* **2023**, *48*, 2861–2875. [CrossRef]

17. Bovo, A.; Poli, N.; Trovò, A.; Marini, G.; Guarnieri, M. Hydrogen energy storage system in a Multi-Technology Microgrid:technical features and performance. *Int. J. Hydrogen Energy* **2023**, *48*, 12072–12088. [CrossRef]
18. Walter, V.; Göransson, L.; Taljegard, M.; Öberg, S.; Odenberger, M. Low-cost hydrogen in the future European electricity system–Enabled by flexibility in time and space. *Appl. Energy* **2023**, *330*, 120315. [CrossRef]
19. National Green Hydrogen Mission. Available online: https://pib.gov.in/PressReleasePage.aspx?PRID=1888547 (accessed on 8 January 2023).
20. Assareh, E.; Dejdar, A.; Ershadi, A.; Jafarian, M.; Mansouri, M.; Roshani, A.S.; Azish, E.; Saedpanah, E.; Lee, M. Techno-economic analysis of combined cooling, heating, and power (CCHP) system integrated with multiple renewable energy sources and energy storage units. *Energy Build.* **2023**, *278*, 120315. [CrossRef]
21. Van, L.P.; Chi, K.D.; Duc, T.N. Review of hydrogen technologies based microgrid: Energy management systems, challenges and future recommendations. *Int. J. Hydrogen Energy* 2023; *in press*. [CrossRef]
22. Pang, K.Y.; Liew, P.Y.; Woon, K.S.; Ho, W.S.; Alwi, S.R.W.; Klemeš, J.J. Multi-period multi-objective optimisation model for multi-energy urban-industrial symbiosis with heat, cooling, power and hydrogen demands. *Energy* **2023**, *262*, 125201. [CrossRef]
23. Sambhi, S.; Sharma, H.; Bhadoria, V.; Kumar, P.; Chaurasia, R.; Chaurasia, G.S.; Fotis, G.; Vita, V.; Ekonomou, L.; Pavlatos, C. Economic Feasibility of a Renewable Integrated Hybrid Power Generation System for a Rural Village of Ladakh. *Energies* **2022**, *15*, 9126. [CrossRef]
24. Zafeiropoulou, M.; Mentis, I.; Sijakovic, N.; Terzic, A.; Fotis, G.; Maris, T.I.; Vita, V.; Zoulias, E.; Ristic, V.; Ekonomou, L. Forecasting Transmission and Distribution System Flexibility Needs for Severe Weather Condition Resilience and Outage Management. *Appl. Sci.* **2022**, *12*, 7334. [CrossRef]
25. Marocco, P.; Ferrero, D.; Lanzini, A.; Santarelli, M. The role of hydrogen in the optimal design of off-grid hybrid renewable energy systems. *J. Energy Storage* **2022**, *46*, 103893. [CrossRef]
26. Arevalo, P.; Benavides, D.; Lata-garcía, J.; Jurado, F. Energy control and size optimization of a hybrid system (photovoltaic-hidrokinetic) using various storage technologies. *Sustain. Cities Soc.* **2020**, *52*, 101773. [CrossRef]
27. Xia, T.; Rezaei, M.; Dampage, U.; Alharbi, S.; Nasif, O.; Borowski, P.; Mohamed, M. Techno-Economic Assessment of a Grid-Independent Hybrid Power Plant for Co-Supplying a Remote Micro-Community with Electricity and Hydrogen. *Processes* **2021**, *9*, 1375. [CrossRef]
28. Wu, Z.; Zhu, P.; Yao, J.; Tan, P.; Xu, H.; Chen, B.; Yang, F.; Zhang, Z.; Ni, M. Thermo-economic modeling and analysis of an NG-fueled SOFC-WGS-TSA-PEMFC hybrid energy conversion system for stationary electricity power generation. *Energy* **2020**, *192*, 116613. [CrossRef]
29. Temiz, M.; Javani, N. Design and analysis of a combined floating photovoltaic system for electricity and hydrogen production. *Int. J. Hydrogen Energy* **2020**, *45*, 3457–3469. [CrossRef]
30. Nasser, M.; Megahed, T.F.; Ookawara, S.; Hassan, H. Performance evaluation of PV panels/wind turbines hybrid system for green hydrogen generation and storage: Energy, exergy, economic, and enviroeconomic. *Energy Convers. Manag.* **2022**, *267*, 115870. [CrossRef]
31. Kamel, A.A.; Rezk, H.; Abdelkareem, M.A. Enhancing the operation of fuel cell-photovoltaic-battery-supercapacitor renewable system through a hybrid energy management strategy. *Int. J. Hydrogen Energy* **2021**, *46*, 6061–6075. [CrossRef]
32. Ghenai, C.; Salameh, T.; Merabet, A. Technico-economic analysis of off grid solar PV/Fuel cell energy system for residential community in desert region. *Int. J. Hydrogen Energy* **2020**, *45*, 11460–11470. [CrossRef]
33. Jahangir, M.H.; Cheraghi, R. Economic and environmental assessment of solar-wind-biomass hybrid renewable energy system supplying rural settlement load. *Sustain. Energy Technol. Assess.* **2020**, *42*, 100895. [CrossRef]
34. Rad, M.A.V.; Ghasempour, R.; Rahdan, P.; Mousavi, S.; Arastounia, M. Techno-economic analysis of a hybrid power system based on the cost-effective hydrogen production method for rural electrification, a case study in Iran. *Energy* **2020**, *190*, 116421. [CrossRef]
35. Cao, Y.; Dhahad, H.A.; Togun, H.; Anqi, A.E.; Farouk, N.; Farhang, B. A novel hybrid biomass-solar driven triple combined power cycle integrated with hydrogen production: Multi-objective optimization based on power cost and CO_2 emission. *Energy Convers. Manag.* **2021**, *234*, 113910. [CrossRef]
36. Rezaei, M.; Naghdi-Khozani, N.; Jafari, N. Wind energy utilization for hydrogen production in an underdeveloped country: An economic investigation. *Renew. Energy* **2020**, *147*, 1044–1057. [CrossRef]
37. Khosravi, A.; Sanna Syri, M.E.H.; Assad, M.M. Thermodynamic and economic analysis of a hybrid ocean thermal energy conversion/photovoltaic system with hydrogen-based energy storage system. *Energy* **2019**, *172*, 304–319. [CrossRef]
38. Singh, S.; Chauhan, P.; Aftab, M.A.; Ali, I.; Hussain, S.M.S.; Ustun, T.S. Cost Optimization of a Stand-Alone Hybrid Energy System with Fuel Cell and PV. *Energies* **2020**, *13*, 1295. [CrossRef]
39. Almutairi, K.; Dehshiri, S.S.H.; Mostafaeipour, A.; Jahangiri, M.; Techato, K. Technical, economic, carbon footprint assessment, and prioritizing stations for hydrogen production using wind energy: A case study. *Energy Strat. Rev.* **2021**, *36*, 100684. [CrossRef]
40. Google Maps. Available online: http://maps.google.com/ (accessed on 10 December 2022).
41. NASA Power—Data Access Viewer. Available online: https://power.larc.nasa.gov/data-access-viewer/ (accessed on 10 ecember 2022).
42. Solar Resource Glossary. Available online: https://www.nrel.gov/grid/solar-resource/solar-glossary.html (accessed on 10 December 2022).

43. Direct Solar Irradiation. Available online: https://www.sciencedirect.com/topics/engineering/direct-normal-irradiation (accessed on 10 December 2022).
44. Sharma, H.; Pal, N.; Kumar, P.; Yadav, A. A control strategy of hybrid solar-wind energy generation system. *Arch. Electr. Eng.* **2017**, *66*, 241–251. [CrossRef]
45. Kumar, P.; Pal, N.; Sharma, H. Techno-economic analysis of solar photo-voltaic/diesel generator hybrid system using different energy storage technologies for isolated islands of India. *J. Energy Storage* **2021**, *41*, 102965. [CrossRef]
46. Kumar, P.; Pal, N.; Sharma, H. Optimization and techno-economic analysis of a solar photo-voltaic/biomass/diesel/battery hybrid off-grid power generation system for rural remote electrification in eastern India. *Energy* **2022**, *247*, 123560. [CrossRef]
47. Kumar, P.; Pal, N.; Sharma, H. Performance analysis and evaluation of 10 kWp solar photovoltaic array for remote islands of Andaman and Nicobar. *Sustain. Energy Technol. Assess.* **2020**, *42*, 100889. [CrossRef]
48. Technology Brief: Analysis of Current-Day Commercial Electrolyzers. Available online: https://www.nrel.gov/docs/fy04osti/36705.pdf (accessed on 15 November 2022).
49. Sorrenti, I.; Zheng, Y.; Singlitico, A.; You, S. Low-carbon and cost-efficient hydrogen optimisation through a grid-connected electrolyser: The case of GreenLab skive. *Renew. Sustain. Energy Rev.* **2023**, *171*, 113033. [CrossRef]
50. Chen, Z.; Yiliang, X.; Hongxia, Z.; Yujie, G.; Xiongwen, Z. Optimal design and performance assessment for a solar powered electricity, heating and hydrogen integrated energy system. *Energy* **2023**, *262*, 125453. [CrossRef]
51. Sijakovic, N.; Terzic, A.; Fotis, G.; Mentis, I.; Zafeiropoulou, M.; Maris, T.I.; Zoulias, E.; Elias, C.; Ristic, V.; Vita, V. Active System Management Approach for Flexibility Services to the Greek Transmission and Distribution System. *Energies* **2022**, *15*, 6134. [CrossRef]
52. Sambhi, S.; Sharma, H.; Bhadoria, V.; Kumar, P.; Chaurasia, R.; Fotis, G.; Vita, V. Technical and Economic Analysis of Solar PV/Diesel Generator Smart Hybrid Power Plant Using Different Battery Storage Technologies for SRM IST, Delhi-NCR Campus. *Sustainability* **2023**, *15*, 3666. [CrossRef]
53. Fotis, G.; Vita, V.; Maris, T.I. Risks in the European Transmission System and a Novel Restoration Strategy for a Power System after a Major Blackout. *Appl. Sci.* **2022**, *13*, 83. [CrossRef]
54. Vita, V.; Fotis, G.; Pavlatos, C.; Mladenov, V. A New Restoration Strategy in Microgrids after a Blackout with Priority in Critical Loads. *Sustainability* **2023**, *15*, 1974. [CrossRef]
55. Wang, Z.; Fang, G.; Wen, X.; Tan, Q.; Zhang, P.; Liu, Z. Coordinated operation of conventional hydropower plants as hybrid pumped storage hydropower with wind and photovoltaic plants. *Energy Convers. Manag.* **2023**, *277*, 116654. [CrossRef]